Two-level systems in fluorite mixed crystals - a far-infrared study

2001 J. Phys.: Condens. Matter 13 2177

(http://iopscience.iop.org/0953-8984/13/10/313)

INSTITUTE OF PHYSICS PUBLISHING JOURNAL OF PHYSICS: CONDENSED MATTER

J. Phys.: Condens. Matter **13** (2001) 2177–2200 www.iop.org/Journals/cm PII: S0953-8984(01)16669-5

Two-level systems in fluorite mixed crystals—a far-infrared study

S A FitzGerald[1], **A J Sievers**[2] **and J A Campbell**[3]

[1] Department of Physics, Oberlin College, Oberlin, OH 44074, USA
[2] Laboratory of Atomic and Solid State Physics and Cornell Center for Materials Research, Cornell University, Ithaca, NY 14853, USA
[3] Department of Physics, University of Canterbury, Christchurch, New Zealand

Received 29 August 2000

Abstract

Low-temperature far-infrared absorption measurements have been made on six different alkaline earth:rare earth fluoride mixed crystal systems at a number of concentrations. All of these chemically disordered crystals display a glass-like continuous distribution of two-level systems (TLS) throughout the millimetre wave spectral region. Much of this study has focused on LaF_3 doping where the effective density of states of the TLS initially increases with dopant concentration, reaching a maximum saturated value at a concentration of about 5 mol% for a CaF_2 host, 20% for SrF_2 and at least 35% for BaF_2. The magnitude of the saturated TLS optical density of states is system dependent, varying from roughly one-fifth to five times that found in a standard soda-lime–silica glass. The optical strength indicates that only a small fraction, less than one in a thousand, of the dopant ions contribute to the TLS optical absorption. At submillimetre wavelengths it is found that both the fluorite mixed crystals and a standard glass exhibit a characteristic temperature-dependent absorption associated with transitions to excited levels above the ground-state TLS manifold. It is proposed that resonant phonon scattering by these excited state transitions is the cause of the plateau observed in the temperature dependence of the thermal conductivity of glasses.

1. Introduction

In 1971 Zeller and Pohl [1] made the first reliable measurements of the anomalous low-temperature heat capacity and thermal conductivity of several glasses. These and subsequent measurements showed that almost all amorphous solids exhibit low-temperature thermal, dielectric and acoustic properties [2–7] very different from those found in dielectric crystals. The most widely accepted phenomenological explanation consistent with the observed properties is described by the two-level systems (TLS) tunnelling model formulated in 1972 by Phillips [8] and, independently, by Anderson *et al* [9]. Because of the random nature of amorphous materials it was proposed that a small fraction of atoms or groups of atoms can tunnel. To account for the data the end result was a near uniform distribution of TLS that dominated the thermodynamic behaviour of amorphous materials at low temperatures.

0953-8984/01/102177+24$30.00

Despite the model's success in reproducing the measured thermal, acoustic and dielectric properties of amorphous materials at low temperatures [2–7], it remains outside the framework of lattice dynamics theory. The fact that this model leaves major fundamental questions on amorphous solids unanswered is a point repeatedly made by Leggett [10]. Specific questions that still remain are the following: why do all amorphous materials appear to have a similar spectral density of TLS, why is the spectral density of states relatively constant and what is the microscopic nature of the tunnelling centres, i.e. what is it that is actually tunnelling in such a diverse range of materials?

One experimental approach to attempt to answer some of these questions for amorphous systems has been to focus on mixed crystal systems. Some mixed crystal systems such as $(ZrO_2)_{1-x}$:$(Y_2O_3)_x$ [11], $(KBr)_{1-x}$:$(KCN)_x$ [12, 13] and $(Ca, Sr, BaF_2)_{1-x}$:$(LaF_3)_x$ [14–20] have been found to contain glass-like distributions of TLS. A continuous distribution of TLS in a dielectric mixed crystal was first observed in the low temperature specific heat of yttrium-stabilized cubic zirconia [11]. The first observation that TLS could be produced in a number of fluorite mixed crystals over a large concentration range was made by Kazanskii using microwave absorption [14]. Subsequent thermal measurements [15] showed that $(BaF_2)_{1-x}$:$(LaF_3)_x$ has a continuous distribution of TLS at low frequencies and that the density of TLS increases with concentration, reaching a maximum value at $x = 0.33$.

In the work presented here, temperature-dependent far-infrared spectroscopy is used to measure systematically the glass-like properties of a number of fluorite mixed crystal systems. This broad band spectroscopic technique extends the accessible energy range of the TLS investigation by more than an order of magnitude relative to other techniques and also provides the needed detailed high-resolution information. The results show that a continuous distribution of TLS exist below 10–20 cm^{-1} for the three systems: BaF_2, SrF_2 and CaF_2, doped with LaF_3. By examining the frequency and concentration dependence of the effective TLS density of states with some care the existence of excited transitions above the ground-state TLS manifold has been identified. The TLS glass-like behaviour is also observed for the mixed crystal systems of CaF_2 doped with YF_3, GdF_3 and LuF_3 and compared with a standard soda-lime–silica (SLS) glass.

In the next section the theoretical connection between a distribution of TLS and the resulting temperature- and frequency-dependent far-infrared absorption is made. The experimental techniques, including both sample preparation and data taking, are discussed in section 3. The results are described in section 4. The results show defect-induced, temperature-independent absorption, and, also, both low-frequency and high-frequency temperature-dependent absorption. The data at the higher frequencies reveal the existence of excited-state transitions. The results are analysed in section 5 in terms of the TLS model from which an effective density of states can be extracted. The effective density of states is shown to increase with dopant concentration before saturating at a value comparable to that of a glass. Finally, it is demonstrated how the existence of the higher-frequency excited-state transitions is a natural consequence of the oscillator strength sum rule. The discussion in section 6 compares the TLS in mixed crystals with those found in glasses, examines the cluster-TLS question, connects the thermal conductivity plateau in glasses to the TLS excited state transitions and, finally, contrasts the far-infrared results for the mixed crystals with those recently observed in Raman measurements.

2. TLS behaviour

The standard TLS model assumes a broad, relatively flat distribution of TLS [9]. There are two possible processes in which such a distribution leads to dielectric absorption: resonance and relaxation. In resonant absorption the far-infrared electric field couples directly to the dipole

moment linking the two levels. This leads to an absorption of a standard form

$$\alpha(\omega, T) = \frac{\hbar\omega}{nc} B_{01} \left(\frac{n^2+2}{3}\right)^2 (N_0 - N_1) \tag{1}$$

where n is the refractive index, c is the velocity of light, $[(n^2+2)/3]^2$ describes the local field correction and B_{01}, the Einstein coefficient, is given by $B_{01} = 8\pi^3|\langle 0|\mu|1\rangle|^2/3h^2$, where $\langle 0|\mu|1\rangle$ is the induced dipole moment linking the two levels. N_0 and N_1 are the population densities per unit frequency in the ground and first excited states, respectively. For resonant absorption only those states with energy splitting $E = \hbar\omega$ will contribute to the absorption at frequency ω. In this case the partition function is simply $Z = 1 + \exp(-\hbar\omega/kT)$. Substituting this result into (1) yields

$$\alpha(\omega, T) = \frac{4\pi^2 n_e(E)|_{E=\hbar\omega}\mu^2}{3nc} \left(\frac{n^2+2}{3}\right)^2 \omega \tanh(\hbar\omega/2kT) \tag{2}$$

where n_e is the optical density of TLS coupling to the electric field. This can be rewritten in a simplified form as

$$\alpha(\omega, T) = G(\omega)\omega \tanh(\hbar\omega/2kT) \tag{3}$$

where, to a first approximation, $G(\omega)$ is taken to be a constant independent of frequency.

In addition to any TLS behaviour, the presence of disorder in a harmonic crystal leads to a relaxation of the phonon selection rules which may produce a large defect-induced, temperature-independent far-infrared absorption [21, 22]. Based on earlier detailed work [21, 23], Bagade and Stolen [22] obtained an expression for the optical absorption induced by N charged defects in a harmonic lattice, namely

$$\alpha(\omega) = \frac{Nq^2}{3\rho nc}\omega^2 \left(\frac{2}{c_t^3} + \frac{1}{c_l^3}\right) \tag{4}$$

where q is the charge, c_t and c_l are the transverse and longitudinal velocities of sound, ρ is the mass density and n and c represent the refractive index and velocity of light, respectively. The dotted curve in figure 1(a) shows the predicted temperature-independent absorption curve, where the relevant physical parameters are taken from [24] for a standard glass. The full curves show the temperature-dependent resonant absorption for five different temperatures as predicted by equation (3) for a distribution of TLS. The harmonic temperature-independent absorption clearly dominates.

In (4) the frequency dependence arises solely from the Debye density of states. It is derived using a very specific model in which it is assumed that all N defect charges act independently without any correlation. A more general model leads to the form [25]

$$\alpha(\omega) = \langle M(\omega, \varepsilon, e^* \ldots) g(\omega)\rangle \tag{5}$$

where M is a generalized coupling coefficient which may depend on several parameters, such as the frequency, an effective disorder-induced charge or the dielectric constant of the medium. All of these factors can lead to a frequency dependence which is more complex than the simple quadratic dependence of (4); however, even in this quite general model the harmonic absorption coefficient is still temperature independent. In practice this large background effect can be subtracted out by examining the temperature-induced change in the absorption relative to that of the reference temperature, so that

$$\Delta\alpha(T; T_R) = \alpha(T) - \alpha(T_R) = -\omega G(\omega)\Delta P(T_R, T) \tag{6}$$

where $\Delta P(T_R, T) \equiv [\tanh(\hbar\omega/2kT_R) - \tanh(\hbar\omega/2kT)]$.

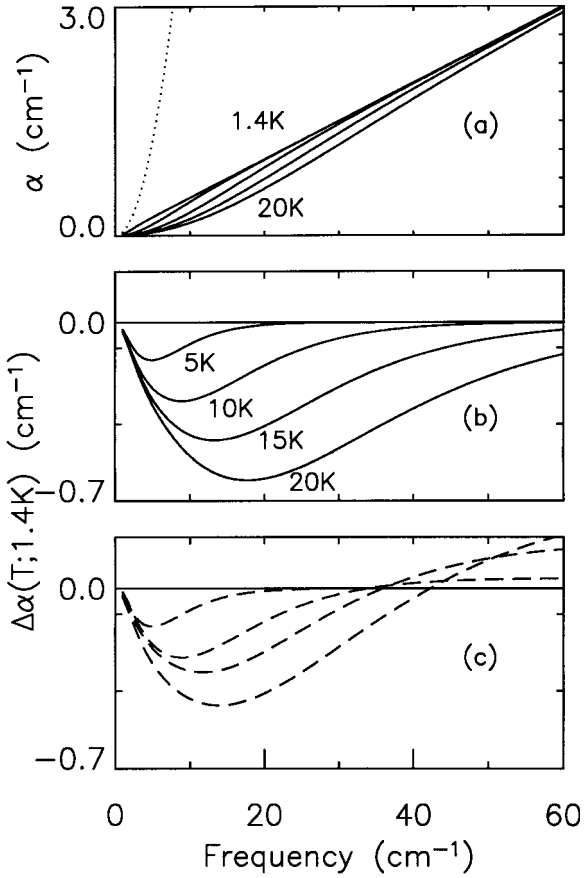

Figure 1. Theoretical predictions for the far-infrared absorption in amorphous materials. The parameters used here are taken from [24]. (a) The resonant absorption for a constant distribution of TLS at temperatures of 1.4, 5, 10, 15 and 20 K. The dotted curve shows a typical temperature-independent absorption for a standard glass. (b) The temperature-induced change in the resonant absorption $\Delta\alpha(T;\ 1.4\,\mathrm{K})$ predicted for a constant distribution of TLS. (c) The complete temperature dependence, $\Delta\alpha(T;\ 1.4\ \mathrm{K})$, including both the relaxation and resonant contributions from a constant distribution of TLS. After [17].

Figure 1(b) shows the temperature-induced change in the absorption for a flat distribution of TLS ($G(\omega) = \text{constant}$) where the reference temperature is taken to be 1.4 K. Note that the TLS absorption always decreases with increasing temperature because increasing the temperature decreases the population difference between the two levels. For TLS with energy splitting $\hbar\omega \gg kT$, the change in temperature has little effect, and hence $\Delta\alpha$ tends to zero.

A distribution of TLS can also produce absorption through relaxation processes. The relaxation absorption for a given frequency ω involves the contribution from all of the TLS, not just those with an energy splitting $E = \hbar\omega$. Phonon-assisted tunnelling leads to an absorption of the form [4]

$$\alpha = \frac{\bar{P}\mu^2}{nc6kT}\int_0^\infty\int_{\tau_{min}}^\infty (1-\tau_{min}/\tau)^{1/2}\,\mathrm{sech}^2\left(\frac{E}{2kT}\right)\frac{\omega^2}{1+\omega^2\tau^2}\,\mathrm{d}\tau\,\mathrm{d}E. \qquad (7)$$

where $\bar{P}$ is the constant spectral density of tunnelling systems per unit asymmetry and overlap parameter, and τ_{min} is the minimum relaxation time for phonon-assisted tunnelling.

In a similar way, phonon-activated relaxation over the potential barriers between wells also leads to an absorption which has contributions from the complete range of the TLS. To account for the distribution of barrier heights, the convention of Hunklinger and von Schickfus [26] is used in which the density of states $n_e \rightarrow \int P(V)\,\mathrm{d}V$, where $P(V)$ is taken to be a Gaussian distribution of barrier heights V. This leads to an absorption coefficient of the form

$$\alpha_{ac} = \frac{\mu^2}{nc3kT}\int_0^{\infty}\int_{V_{min}}^{V_{max}} P(V)\,\mathrm{sech}^2\left(\frac{E}{2kT}\right)\frac{\omega^2\tau(V)}{1+\omega^2\tau(V)^2}\,\mathrm{d}V\,\mathrm{d}E$$
$$= \frac{2\pi\mu^2}{3nc}\int_{V_{min}}^{V_{max}} P(V)\frac{\omega^2\tau(V)}{1+\omega^2\tau(V)^2}\,\mathrm{d}V \qquad (8)$$

where the activation relaxation time, τ, is now a function of the barrier height:

$$\tau^{-1}(V) = \omega_0 \exp(-V/kT) \qquad (9)$$

and ω_0 is an attempt frequency, normally assumed to be $\sim 10^{13}$ s^{-1} [26].

Figure 1(c) shows the complete TLS model predictions including both resonance and relaxation absorption. The relevant parameters are taken from [24]. For temperatures below 10 K the curves show little difference from those of resonant absorption alone since the relaxation contribution is quenched, but at higher temperatures the contributions from the relaxation mechanisms become significant. When these relaxation terms dominate $\Delta\alpha(T;\ 1.4\ \mathrm{K})$ becomes positive. Note the characteristic signature for relaxation is that with increasing temperature the $\Delta\alpha(T;\ 1.4\ \mathrm{K})$ curves cross zero at progressively higher frequencies and then asymptotically approach some constant positive value for very high frequencies.

3. Experimental methods

The existence of TLS in the fluorite mixed crystals offers a unique opportunity for studying glass-like properties since large single crystals can be grown readily for rare earth concentrations up to 50 mol% ($x = 0.5$). The fact that CaF_2, SrF_2 and BaF_2 have the same lattice structure combined with the availability of chemically similar rare earth and rare earth-like dopant ions ranging from Y ($Z = 39$) to Lu ($Z = 71$) leads to a large number of possible fluorite mixed crystal systems. Although the ions are chemically similar they differ over a broad range of mass, ionic radius and polarizability, which should impact the dominant defect structure [27].

Single-crystal rods of doped fluorite crystals, 1 cm in diameter and up to 50 mm long, were grown at Canterbury by the Stockbarger technique; in graphite crucibles under vacuum, with PbF_2 as an oxygen getter, using the phase diagrams of Roth *et al* [28] and growth rates of a few to 12 mm h^{-1}. The dopant concentration of the samples was checked using x-ray fluorescence which showed up to a 10% gradient in the concentration along a 5 cm boule. The fluorite cleavage planes and Laue x-ray diffraction confirmed that the samples were indeed single crystals.

Far-infrared transmission spectra were measured over the range 3–40 cm^{-1} using a lamellar grating interferometer in conjunction with a He^3 cooled bolometer detector. All spectra presented here have a resolution of 1 or 1.5 cm^{-1}. Up to five samples could be immersed in pumped liquid helium at 1.4 K. The samples could then, later, be heated using a small heater attached to the copper sample holder. The temperature was monitored with a carbon resistor thermometer. Accurate measurement and temperature control during a scan is crucial. In one test a thermometer mounted inside a mixed crystal sample showed that the temperature

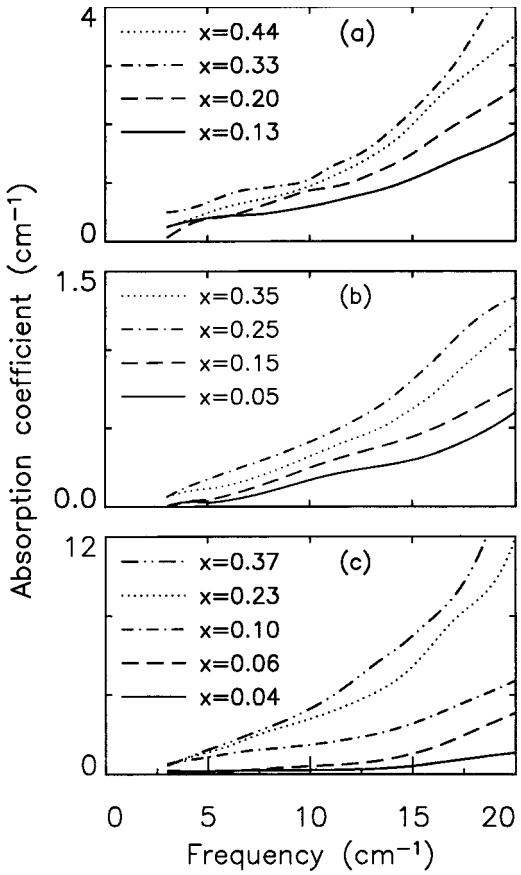

Figure 2. Low-temperature impurity-induced absorption coefficient as a function of frequency and concentration for three different mixed fluorite crystal systems with the same dopant ion. (a) CaF_2, (b) SrF_2 and (c) BaF_2. The LaF_3 concentration ranges from $0.05 \leqslant x \leqslant 0.44$. The temperature is 1.4 K and the resolution is 1.5 cm^{-1}.

of the sample and the temperature of the copper sample holder thermometer agreed to within 0.1 K. For higher frequencies (15–50 cm^{-1}) a Bomem DA3 Michelson interferometer was used together with a 1.6 K composite Si bolometer. For this arrangement the lowest sample temperature was 4.2 K.

4. Results

4.1. Temperature independent absorption

Figure 2 shows the 1.4 K low-frequency absorption coefficient for three different host systems, CaF_2, SrF_2 and BaF_2, as a function of the LaF_3 concentration. In all cases the absorption increases roughly quadratically with the frequency, as expected from (4). The results for $(CaF_2)_{1-x}$:$(LaF_3)_x$, figure 2(a), and $(SrF_2)_{1-x}$:$(LaF_3)_x$, figure 2(b), are quite similar. Both show an absorption whose magnitude increases steadily with concentration up to a maximum at $x \sim 0.25$–0.35. The results for $(BaF_2)_{1-x}$:$(LaF_3)_x$, figure 2(c), show a slightly stronger concentration dependence which continues to increase even at the highest measured concentration of $x = 0.37$.

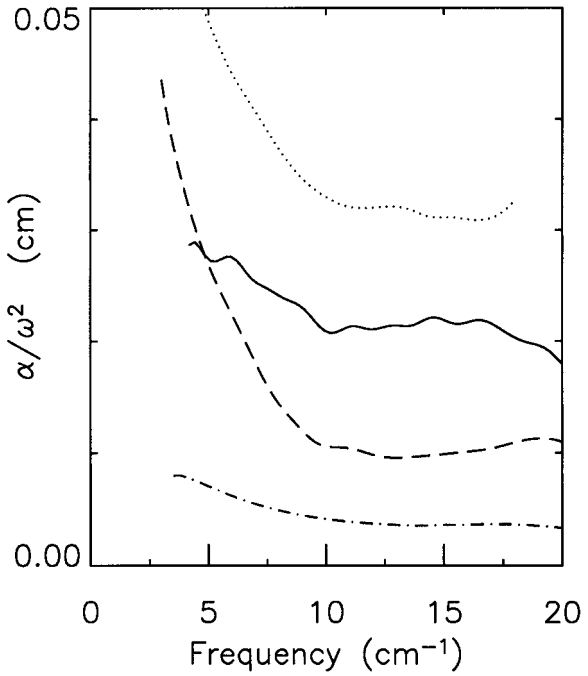

Figure 3. Low-temperature absorption coefficient divided by the frequency squared against frequency for three mixed crystals and SLS glass at 1.4 K. The dotted curve denotes $(BaF_2)_{0.63}$:$(LaF_3)_{0.37}$, the dashed curve denotes $(CaF_2)_{0.67}$:$(LaF_3)_{0.33}$, the dot–dashed curve denotes $(SrF_2)_{0.65}$:$(LaF_3)_{0.35}$ and the full curve denotes the SLS glass. The resolution is 1.5 cm^{-1}.

To separate the disorder-induced phonon term (equation (4)) from the resonant absorption at low temperatures (equation (3) where $\tanh(\hbar\omega/2kT) \rightarrow 1$) an $\alpha(\omega)/\omega^2$ against ω plot is helpful. Figure 3 shows the results for a high concentration of LaF_3 in the three mixed crystal hosts and, for comparison, the results for the SLS glass. At the higher frequencies above 10 cm^{-1} the disorder term dominates since the data are essentially constant against frequency, while for lower frequencies the $1/\omega$ dependence demonstrates that the resonant TLS absorption term becomes important. For the $(CaF_2)_{0.67}$:$(LaF_3)_{0.33}$ and the $(BaF_2)_{0.63}$:$(LaF_3)_{0.37}$ systems the relative contribution from the TLS absorption is quite strong. For the latter case it should be noted that both components to the absorption are stronger than observed for a standard SLS glass. In contrast, the respective pure crystals do not absorb on this scale at these frequencies since the difference phonon bands are quenched at low temperatures [29].

4.2. Temperature dependence

Figure 4 presents the temperature-dependent absorption spectrum of $(CaF_2)_{0.8}$:$(LaF_3)_{0.2}$ in the far-infrared spectral region. At low frequencies the largest absorption occurs at the lowest temperatures. With increasing temperature the magnitude of the absorption coefficient decreases, reaching a minimum at about 15 K, and then increases again at higher temperatures. For frequencies above 20 cm^{-1} the relative change in the absorption coefficient with temperature is quite small. This general form of the temperature dependence has been found previously in standard glasses [24] and follows the predictions of the TLS model

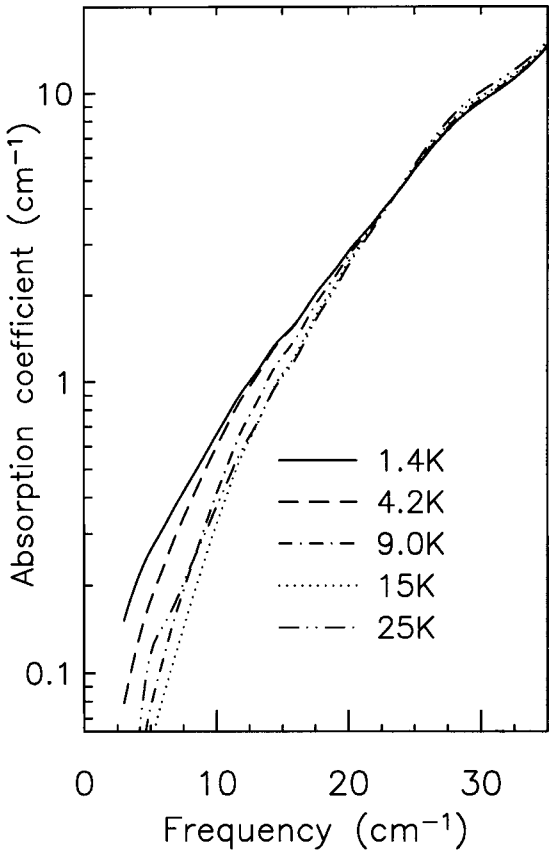

Figure 4. Temperature dependence of the absorption coefficient for $(CaF_2)_{0.8}$:$(LaF_3)_{0.2}$ against frequency. For frequencies below 20 cm^{-1} the absorption goes through a minimum value at 15 K, as the temperature increases, very similarly to that observed for a standard SLS glass. After [16].

presented in section 2. The temperature-dependent spectral data for the other fluorite mixed crystals are qualitatively similar to those shown here.

The temperature-induced change in the absorption coefficient for a representative sample of the three host systems is displayed in figure 5. The temperature is varied from 1.4 to 25 K in each case. Figure 5(a) shows the results for $(CaF_2)_{0.8}$:$(LaF_2)_{0.2}$. The negative peak in $\Delta\alpha(T;\ 1.4\ \mathrm{K})$ grows and shifts to higher frequencies with increasing temperatures. The $\Delta\alpha$ reaches a minimum at 19 K and starts to increase for higher temperatures. Figure 5(b) shows the data for $(SrF_2)_{0.75}$:$(LaF_3)_{0.25}$. Here $\Delta\alpha$ reaches a minimum value at 15 K. For $(BaF_2)_{0.77}$:$(LaF_3)_{0.23}$, figure 5(c), the turn-around in $\Delta\alpha$ is even more dramatic, by 25 K $\Delta\alpha$ has increased to a value larger than that at 4 K. Clearly, although resonant TLS absorption is dominant at low temperatures, it is not the only process occurring at higher temperatures. The overall nature of the temperature dependence for the three mixed crystal systems is qualitatively similar with the curves being shifted somewhat in frequency from one system to another.

Even for the lower temperatures the shape of the $\Delta\alpha(T;\ 1.4\ \mathrm{K})$ at higher frequencies is quite different from the resonant TLS predictions summarized in figure 1(a). Deviations from the resonant model have been described in a previous far-infrared study [24] on standard glasses, and these were explained by the inclusion of the relaxation absorption presented in

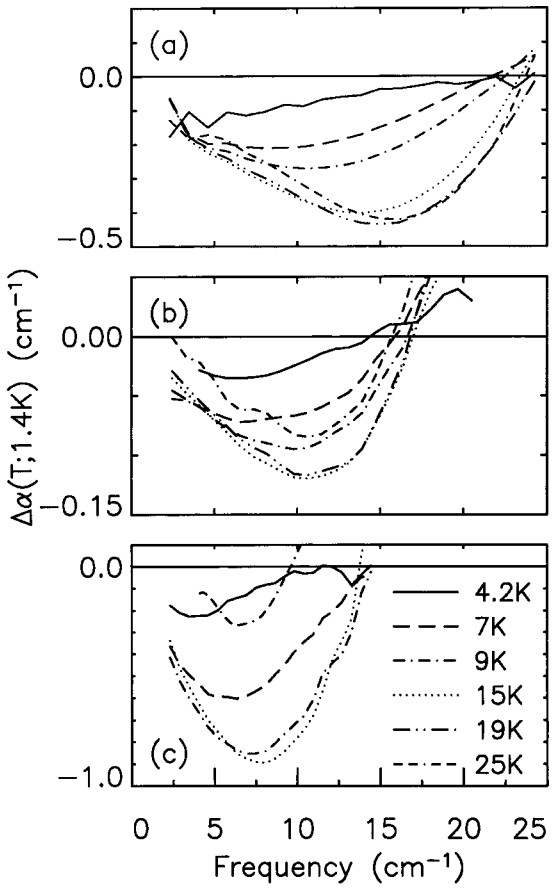

Figure 5. The temperature-induced change in absorption coefficient $\Delta\alpha(T;\ 1.4\ \mathrm{K})$ against frequency for three different $(AF_2)_{1-x}$:$(LaF_3)_x$ systems. (a) $(CaF_2)_{0.8}$:$(LaF_3)_{0.2}$, (b) $(SrF_2)_{0.75}$:$(LaF_3)_{0.25}$ and (c) $(BaF_2)_{0.77}$:$(LaF_3)_{0.23}$. Note the similarity of the temperature dependence for the three different systems with the same dopant ion although each has its own characteristic zero-crossing frequency.

figure 1(c). This earlier data, however, only extended out to 15 cm^{-1}, and it proved impossible for this model to achieve satisfactory agreement at different temperatures.

In the present case, with the data extending to somewhat higher frequencies, the addition of relaxation absorption cannot provide a complete explanation of the observed temperature dependence. In figure 5 the frequency at which the $\Delta\alpha(T;\ 1.4\ \mathrm{K})$ curves cross zero shows relatively little change with temperature. The crossing frequency is smallest for the smallest temperature interval, reaches it highest value in the region of 15–19 K and then shifts back to lower frequencies for higher temperatures. Over the entire temperature region studied the shift in the crossing frequency is surprisingly small, being no more than 5–15% depending on the host lattice. In contrast, the zero-crossing for the theoretical curves shown in figure 1(c), which are controlled by the relaxation absorption contribution, shift by almost 100% over the same temperature interval.

The concentration dependence of the temperature-induced change in the absorption coefficient provides another way to examine the TLS signature. Figure 6 shows the change in absorption, $\Delta\alpha(9\ \mathrm{K};\ 1.4\ \mathrm{K})$, over the complete concentration range measured for all

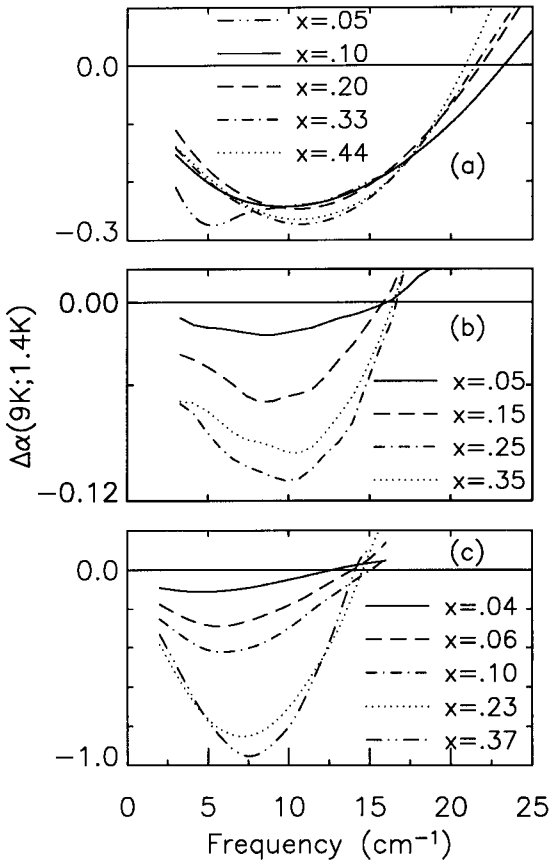

Figure 6. The temperature-induced change in the absorption coefficient $\Delta\alpha$(9 K; 1.4 K) against frequency for three different mixed crystal $(AF_2)_{1-x}$:$(LaF_3)_x$ systems as a function of concentration. (a) $(CaF_2)_{1-x}$:$(LaF_3)_x$, (b) $(SrF_2)_{1-x}$:$(LaF_3)_x$ and (c) $(BaF_2)_{1-x}$:$(LaF_3)_x$. In each case the frequency dependence of the absorption change is nearly independent of concentration. The resolution is 1 cm^{-1}.

three host systems. Figure 6(a), for the $(CaF_2)_{1-x}$:$(LaF_3)_x$ system, displays a very small concentration dependence over the range of x values shown. For $x = 0.05$ there is evidence for a sharp feature at 5 cm^{-1}. This feature dominates the spectrum at much lower concentrations ($x < 0.001$) which is the subject of a separate impurity-mode study [30]. For figure 6(b), the $(SrF_2)_{1-x}$:$(LaF_3)_x$ system, the magnitude of the absorption change increases steadily with concentration up to $x = 0.25$ and then is reduced for $x = 0.35$. Finally the $(BaF_2)_{1-x}$:$(LaF_3)_x$ system, figure 6(c), shows an absorption change which continues to increases in magnitude with concentration for all the samples examined. Note that even though the magnitude of the effect may change dramatically with concentration, the zero-crossing frequency remains relatively constant for all three hosts, varying by less than 10% over the complete concentration range studied. The crossing frequency does, however, depend on the host cation type, being 22 cm^{-1} for CaF_2, 16 cm^{-1} for SrF_2 and 13.5 cm^{-1} for BaF_2.

Figure 7 shows $\Delta\alpha$(9 K; 1.4 K) for six different systems plus the standard SLS glass. In terms of both magnitude and frequency dependence the glass lies in the middle of the range of values for the mixed crystals. These data demonstrate that the crossing point in $\Delta\alpha$ depends

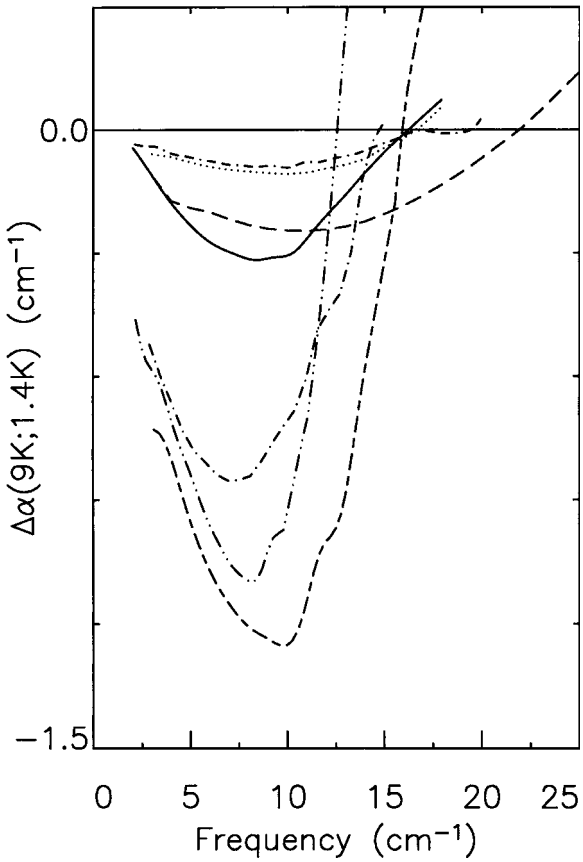

Figure 7. The temperature-induced change in the absorption coefficient $\Delta\alpha$(9 K; 1.4 K) against frequency for six different mixed fluorite systems and SLS glass. The systems are identified as follows: the dash–dash–dot curve denotes $(CaF_2)_{0.9}$:$(GdF_3)_{0.1}$, the dotted curve denotes $(SrF_2)_{0.75}$:$(LaF_3)_{0.25}$, the dashed curve denotes $(CaF_2)_{0.8}$:$(LaF_3)_{0.2}$, the full curve denotes the SLS glass, the dash–dot curve denotes $(BaF_2)_{0.63}$:$(LaF_3)_{0.37}$, the dash–dot–dot curve denotes $(CaF_2)_{0.91}$:$(LuF_3)_{0.09}$ and the long dash–short dash curve denotes $(CaF_2)_{0.91}$:$(YF_3)_{0.09}$. Note that the zero-crossing frequency depends on the dopant ion as well as on the host lattice. The resolution is 1 cm^{-1}.

both on the host system and the dopant ion. A comparison of these results with those presented in figure 3 shows that there is a correlation between the total defect-induced absorption and the temperature-induced change in absorption. All the mixed crystals that display a large temperature-independent absorption also show an proportionally large temperature-dependent change in absorption.

For completeness mixed crystals of the form $(AF_2)_{1-x}$:$(A'F_2)_x$ where A, A′ = Ca, Sr or Ba were also examined. Both $(CaF_2)_{0.7}$:$(BaF_2)_{0.3}$ and $(BaF_2)_{0.7}$:$(SrF_2)_{0.3}$ show no temperature-induced change in absorption for $T < 25$ K within the instrumental noise level. Hence the magnitude of any absorption change is at least a factor of 100 smaller than that of samples doped with the same concentration of LaF_3. Similarly the temperature-independent absorption for $(AF_2)_{1-x}$:$(A'F_2)_x$ samples is also greatly reduced. At 1.4 K $(CaF_2)_{0.7}$:$(BaF_2)_{0.3}$ has an absorption spectrum which has a similar shape, but is reduced by a factor of about 50 relative to that of $(CaF_2)_{0.73}$:$(LaF_3)_{0.33}$.

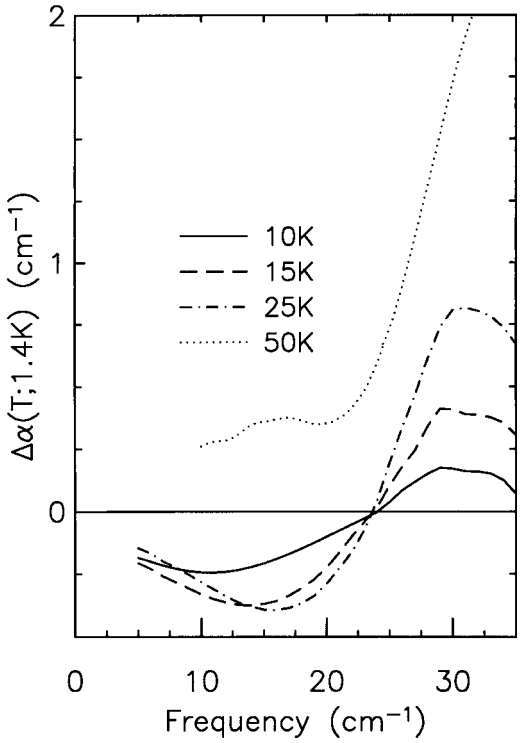

Figure 8. Change in absorption coefficient for $(CaF_2)_{0.8}$:$(LaF_3)_{0.2}$ against frequency over an extended frequency region. Note that at temperatures of 25 K and below all the curves cross zero at almost the same frequency. At higher temperatures thermally activated relaxation processes becomes important. The resolution is 1.5 cm^{-1}.

4.3. High-frequency temperature dependence

Figure 8 presents the change in absorption $\Delta\alpha(T;\ 1.4\ \mathrm{K})$ against frequency for $(CaF_2)_{0.8}$:$(LaF_3)_{0.2}$ up to 50 K. For frequencies below 22 cm^{-1} the absorption coefficient initially decreases with increasing temperature, as described earlier, but by 50 K a dramatic increase in absorption occurs at all frequencies. This increase could be due to the thermally activated TLS relaxation processes described earlier or the result of anharmonic difference band absorption processes involving crystal phonon modes [29]. Since difference band processes should be equally likely in low-concentration samples or pure crystals and since our measurements for low concentrations show no sign of any thermally-activated absorption below about 50 K, the large absorption increase with temperature in high-concentration samples is assigned to thermally-activated TLS relaxation absorption. The discussion below is restricted to data taken at temperatures of 15 K or lower where these high-temperature thermal relaxation processes remain quenched.

At low temperatures the $\Delta\alpha(T;\ 1.4\ \mathrm{K})$ curves shown in figure 8 are positive for frequencies above 22 cm^{-1}, peak at roughly 31 cm^{-1} and then decrease again with increasing frequency. This final return to a temperature-independent behaviour at a particular frequency is an important signature since it cannot be accounted for solely by the relaxation processes. The theoretical curves shown in figure 1(c) demonstrate that the relaxation terms lead to $\Delta\alpha(T;\ 1.4\ \mathrm{K})$ becoming positive and constant at higher frequencies. To determine whether

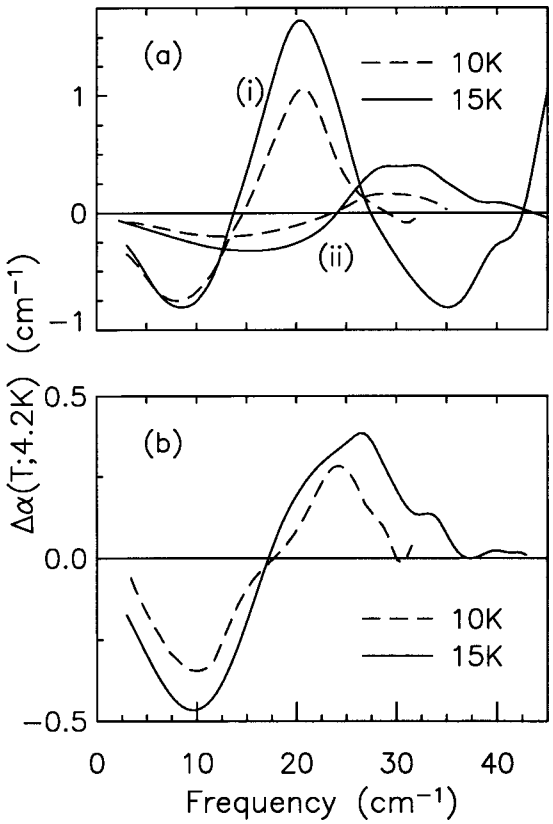

Figure 9. The temperature-induced changes in the absorption coefficient against frequency in mixed crystals and glasses over an extended frequency interval. For each sample $\Delta\alpha$(10 K; 4.2 K) (broken curve) and $\Delta\alpha$(15 K; 4.2 K) (full curve) are shown. (a) (i) $(BaF_2)_{0.77}$:$(LaF_3)_{0.23}$ and (ii) $(CaF_2)_{0.87}$:$(LaF_3)_{0.13}$. (b) the SLS glass. Note that the zero crossing at 17 cm^{-1} for the SLS glass is nearly independent of temperature, just as for the mixed crystal data. After [16].

the positive peak in the $\Delta\alpha(T;\ 1.4\ \mathrm{K})$ is unique to the $(CaF_2)_{1-x}$:$(LaF_3)_x$ system or a general feature of these mixed crystals, another mixed crystal system, $(BaF_2)_{1-x}$:$(LaF_3)_x$ is also measured in the high frequency region.

Figure 9(a) displays $\Delta\alpha(T;\ 1.4\ \mathrm{K})$ for $(BaF_2)_{0.77}$:$(LaF_3)_{0.23}$ (full and broken curves labelled (i)) and $(CaF_2)_{0.87}$:$(LaF_3)_{0.13}$ (full and broken curves labelled (ii)) over the entire frequency interval examined. Note that the reference temperature is now 4.2 K, due to instrumentation constraints at these higher frequencies. The alternating negative and positive nature of the temperature dependence of $\Delta\alpha$ stands out for both mixed crystal systems. Because of the small zero-crossing frequencies of the mixed BaF_2 system, see curves (i), a larger fraction of the higher-frequency excited-state interval is exposed. Two additional zero crossings occur in $\Delta\alpha$, near 27 and 43 cm^{-1}. At still higher frequencies the relative size of the temperature-induced effect becomes too small to measure relative to the increasing temperature-independent absorption, even though on the $\Delta\alpha$ scale in figure 9(a) the magnitude of the peak in each frequency interval remains comparable. The results for the CaF_2 system are similar: see curves (ii) in figure 9(a). Because of the larger characteristic frequency of the first zero crossing only one additional crossing near 43 cm^{-1} has been identified in $\Delta\alpha$(15 K; 4.2 K) before this crystal becomes opaque.

The unusual spectral signature observed here for the mixed fluorite crystals has encouraged us to perform similar high-frequency temperature-dependent measurements on a standard SLS glass. Figure 9(b) shows $\Delta\alpha(T;\ 4.2\ \mathrm{K})$ for this glass. For both 10 and 15 K relative to the 4.2 K reference temperature $\Delta\alpha$ is initially negative, crosses zero at approximately 17 cm^{-1}, becomes positive in an intermediate frequency region and then returns to zero at between 30 and 37 cm^{-1}. At higher frequencies the glass becomes too opaque to determine the temperature-dependent signature. In each of the spectra shown in figure 9 the positive and negative $\Delta\alpha$ areas are the same within the experimental uncertainty.

5. Analysis

5.1. TLS behaviour

Because of the zero crossings in the high-frequency data presented in figure 9 it is clear that there is more than resonant absorption from a distribution of TLS. The first step in the analysis is to determine how well the TLS model fits the data at frequencies below the first zero crossing, i.e. how well (2) describes the experimental data. Although it is now evident that both the dipole moment, μ, and $n_e(\omega)$ appear to vary over the frequency range examined so that $G(\omega)$ is frequency dependent, still the TLS absorption evaluated at any particular frequency must follow the temperature dependence predicted by equation (6).

The low frequency data for $(CaF_2)_{0.9}$:$(LaF_3)_{0.1}$ and for $(CaF_2)_{0.9}$:$(LuF_3)_{0.1}$ are plotted in figures 10 and 11 using the (6) format. Analysis of the low-frequency data for all the $(AF_2)_{1-x}$:$(RF_3)_x$ systems demonstrates that these results are typical. The full lines shown are the predicted response from (6) with the reference temperature $T_R = 1.4$ K. The data for each frequency are extracted from a series of absorption spectra taken at discrete temperatures ranging from 3 to 10 K. The origin for each frequency curve has been displaced for clarity. If the resonant TLS dominates then with no adjustable parameters the temperature-dependent experimental data must follow these straight lines. The slope of each straight line gives $G(\omega)$ at that frequency. The overall agreement between the data and theory is quite good here and for all the systems studied. The conclusion is that the temperature-dependent, low-frequency absorption from 3 to 9 cm^{-1} of fluorite mixed crystals is associated with a broad distribution of TLS.

Figure 12 summarizes the results for $G(\omega)$ plotted as a function of frequency for six different fluorite mixed crystal systems plus the SLS glass. The smallest values, represented by the crosses, are associated with $(SrF_2)_{0.75}$:$(LaF_3)_{0.25}$ while the largest, the solid triangles and squares, come from $(CaF_2)_{0.90}$:$(LuF_3)_{0.10}$ and $(CaF_2)_{0.91}$:$(YF_3)_{0.09}$, respectively. Both $(CaF_2)_{0.87}$:$(LaF_3)_{0.13}$, open squares, and $(BaF_2)_{0.90}$:$(LaF_3)_{0.10}$, open circles, have values comparable to those found for SLS glass (stars). In addition, for these two mixed crystal systems $G(\omega)$ is observed to decrease with increasing frequency over the range of concentrations studied, an interesting result since clustering is expected to play a different role in each system [31]. For any particular $(AF2)_{1-x}(RF_3)_x$ system the results are that the frequency dependence of $G(\omega)$ is largely independent of concentration.

Figure 13 shows the values for $G(\omega)$ plotted as a function of concentration for the three host lattices doped with LaF_3. In all cases the TLS density saturates with increasing concentration. For the $(CaF_2)_{1-x}$:$(LaF_3)_x$ system $G(\omega)$ is essentially independent of concentration (within the scatter of the data) for x greater than 0.05. In contrast, the $(BaF_2)_{1-x}$:$(LaF_3)_x$ system shows a concentration dependence in which $G(\omega)$ is still increasing with concentration even above $x = 0.30$. The $(SrF_2)_{1_x}$:$(LaF_3)_x$ system forms the intermediate case, in which $G(\omega)$ reaches its saturated value somewhere in the region of $x = 0.25$. The detailed results are summarized in table 1.

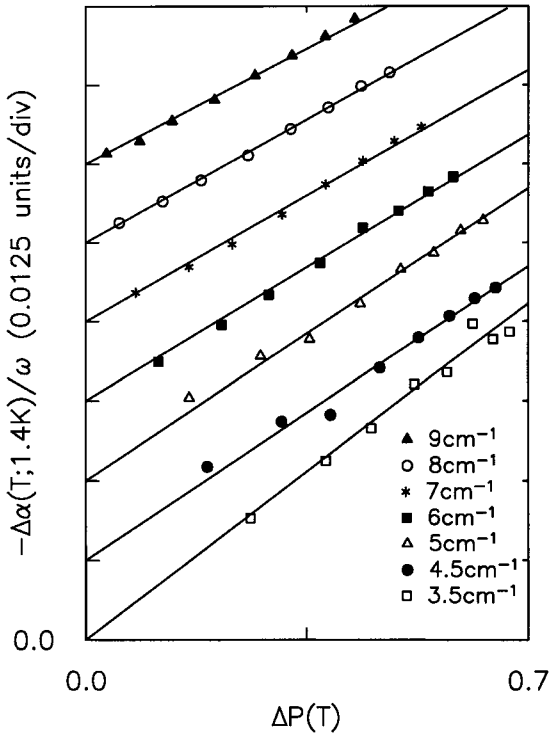

Figure 10. Comparison of theory and experiment for the thermal population of the TLS in $(CaF_2)_{0.9}$:$(LaF_3)_{0.1}$. The full lines show the predictions of equation (6). The reference temperature is 1.4 K. Spectra were taken at 3.2, 4.2, 5.0, 6.0, 7.0, 8.0, 9.0 and 10 K. The data are shown for seven frequencies between 3 and 9 cm^{-1}. In each case the origin has been displaced for clarity and each line represents the best linear fit which passes through the origin.

Table 1. Spectral characteristics for $(AF_2)_{1-x}$:$(RF_3)_x$ fluorite mixed crystal systems. The SLS glass values are also shown. G_{sat} is the value of $G(\omega)$ evaluated at 6 cm^{-1} for a saturated concentration. *Slope* indicates the percentage change in $G(\omega)$ from 3 to 9 cm^{-1}. x_{sat} is the dopant concentration at which $G(6\ cm^{-1})$ approaches its maximum value. Z_c is the frequency (cm^{-1}) at which the $\Delta\alpha(T;\ 1.4\ K)$ curve shows the first zero crossing. *Thermal* refers to a high-temperature thermal cycling effect. The quantity $n_e\mu^2$ was evaluated at 6 cm^{-1}.

Sample	G_{sat}	Slope (%)	x_{sat}	Z_c	Thermal	$n_e\mu^2$
CaF_2–LaF_3	0.055	−25	∼0.05	22	No	1.3×10^{-3}
SrF_2–LaF_3	0.020	+16	∼0.20	16	No	5.0×10^{-4}
BaF_2–LaF_3	0.24	−50	⩾0.35	13.5	No	6.1×10^{-3}
CaF_2–GdF_3	0.024	+14	—	13–20	No	6.1×10^{-4}
CaF_2–YF_3	0.33	+12	∼0.05[a]	15.5	Yes	7.5×10^{-3}
CaF_2–LuF_2	0.31	19	—	12.5	Yes	7.3×10^{-3}
SLS	—	12	—	17	—	2.0×10^{-3}

[a] This is the value for the as-grown sample.

In the case of the $(CaF_2)_{1-x}$:$(LaF_3)_x$ system, the concentration dependence can be well represented by the empirical relation

$$G(\omega) = G_{sat}[1 - \exp(-x/x_{sat})] \tag{10}$$

where G_{sat} is the maximum value of $G(\omega)$ and x_{sat} is the concentration at which the density

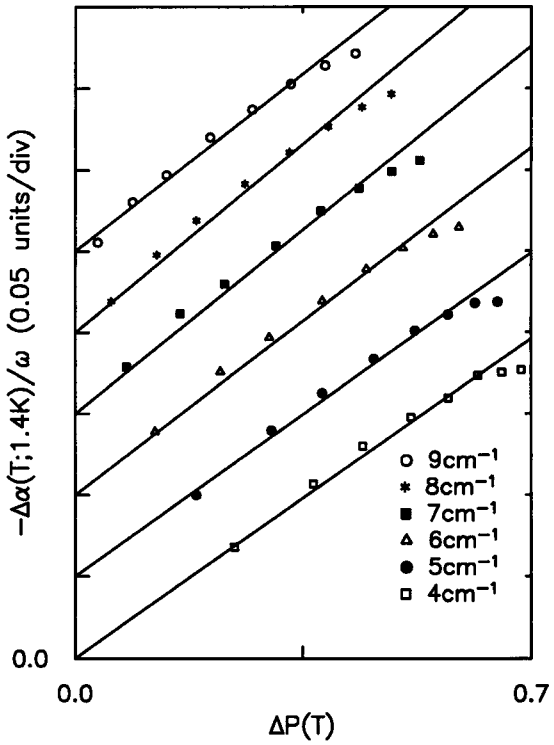

Figure 11. Comparison of theory and experiment for the thermal population of the TLS in $(CaF_2)_{0.9}$:$(LuF_3)_{0.1}$. The full lines show the predictions of equation (6). The reference temperature is 1.4 K. Spectra were taken at 3.2, 4.2, 5.0, 6.0, 7.0, 8.0, 9.0 and 10 K. The data are shown for seven frequencies between 3 and 9 cm^{-1}. In each case the origin has been displaced for clarity and each line represents the best linear fit which passes through the origin.

of the TLS begins to saturate. The data show a linear dependence at the lowest dopant concentration. In contrast, the $(BaF_2)_{1-x}$:$(LaF_3)_x$, and $(SrF_2)_{1-x}$:$(LaF_3)_x$ systems appear to have a small, but non-zero, threshold concentration for the onset of the TLS behaviour.

5.2. Beyond TLS behaviour

Figures 5–7 illustrate that each of these mixed crystal systems and also the SLS glass has a unique frequency at which almost no temperature dependence is observed in $\Delta\alpha$. A possible explanation is that a sudden cutoff in the TLS density of states occurs. It is physically sensible that a flat distribution of the TLS tunnelling states must have an upper bound at some frequency. Figure 14 shows the predicted absorption for the same model parameters used earlier in figure 1, but now in figure 14(a) shows the results for an additional constraint of a sharp cutoff at 13 cm^{-1} in the TLS density of states. This model succeeds in producing a unique frequency for the zero crossing of the $\Delta\alpha(T;\ 1.4\ \mathrm{K})$ curves, as shown in figure 14(c). At the same time, the total absorption, shown in figure 14(b) remains relatively smooth in agreement with our data. However, the addition of a TLS cutoff fails to explain the results of figure 9 where more than one frequency crossing for $\Delta\alpha(T;\ 1.4\ \mathrm{K})$ is observed.

The data for all three systems, two mixed crystals and the SLS glass, presented in figure 9, exhibit a remarkably similar temperature-induced change in absorption at low temperatures.

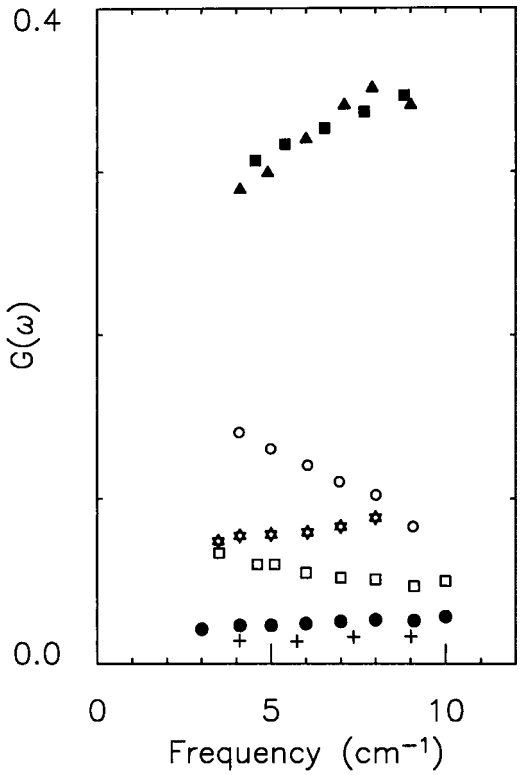

Figure 12. Normalized value of $G(\omega)$ against frequency for six mixed fluorite crystals plus the SLS glass: the full triangles denote $(CaF_2)_{0.91}$:$(LuF_3)_{0.09}$, the full squares denote $(CaF_2)_{0.91}$:$(YF_3)_{0.09}$, the open circles denote $(BaF_2)_{0.9}$:$(LaF_3)_{0.1}$, the stars denote the SLS glass, the open squares denote $(CaF_2)_{0.87}$:$(LaF_3)_{0.13}$, the full circles denote $(CaF_2)_{0.9}$:$(GdF_3)_{0.1}$ and the crosses denote $(SrF_2)_{0.75}$:$(LaF_3)_{0.25}$.

In each case the $\Delta\alpha(T;\ 1.4\ \mathrm{K})$ curves consist of a characteristic S-shape; the temperature dependence alternates from being negative to positive and then back to zero. There is a striking periodicity to this frequency-dependent behaviour which cannot be explained by combining the existing models involving TLS resonant and relaxation absorption [24, 32].

Although it is to be expected that there may be excited energy states above the TLS manifold it has traditionally been assumed that they are at high enough energy that the low-temperature dynamics of the system can be well approximated by just the two lowest levels. The high-frequency temperature-dependent data presented in figure 9 are consistent with the direct probing of excited states above the TLS manifold [16]. The change in sign of $\Delta\alpha$ at the higher frequencies is a natural consequence of the oscillator strength sum rule which states that [33]

$$\int \alpha(\omega, T)\,\mathrm{d}\omega = \text{constant}. \tag{11}$$

This sum rule is quite general and applies to any arbitrary anharmonic arrangement of levels, including those involving tunnelling. According to (11) if the absorption coefficient decreases in one frequency interval then there must be a corresponding increase in its value at other frequencies. Note that KCl:Li^+ is a simple crystalline defect tunnelling system which demonstrates this excited-state effect; namely, an increase in the excited-state absorption coefficient with increased temperature at very low temperatures (see figure 4 in [34]).

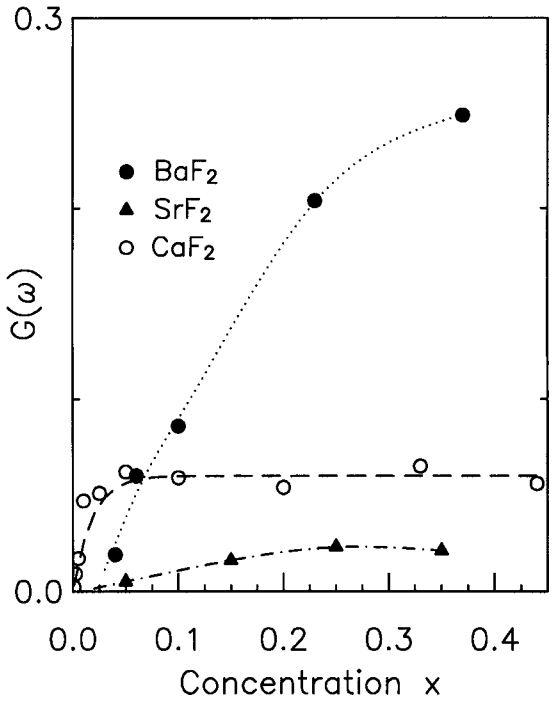

Figure 13. Concentration dependence of $G(\omega)$ for La^{3+} in three host lattices. The full circles denote $(BaF_2)_{1-x}$:$(LaF_3)_x$, the open circles denote $(CaF_2)_{1-x}$:$(LaF_3)_x$ and the full triangles denote $(SrF_2)_{1-x}$:$(LaF_3)_x$. The lines are guides to the eye.

From this perspective the only apparent difference for the mixed crystal cases considered here is that now a broad band of tunnelling transitions decrease in strength with increasing temperature, while at the same time, because of the oscillator strength sum rule, the absorption coefficient for a band of TLS excited-state transitions must increase by a corresponding amount. The result is a change of equal spectral area, but opposite sign. Inspection of figure 9 shows that for all three systems the positive and negative areas of the $\Delta\alpha(T;\ 1.4\ \mathrm{K})$ curves are in fact roughly equal, supporting the idea of the TLS manifold having excited-state transitions. An interesting discovery is that the excited-state transitions are not that far in frequency from the ground-state manifold and hence would be expected to influence transport properties.

6. Discussion

6.1. Comparing TLS in mixed crystals and glasses

Is there a common origin to the far-infrared TLS absorption of the standard SLS glass and the various fluorite mixed crystal systems that have been examined here? Starting with the temperature-independent absorption, the results show that the fluorite mixed crystals plus the SLS glass all possess a 1.4 K absorption which scales roughly quadratically with frequency. Each mixed crystal system shows the same behaviour of a temperature-independent absorption, which initially increases with dopant concentration but then levels off at higher values. Figure 7 confirms that those systems which have a large temperature-independent absorption show a proportionally large temperature-dependent absorption at low temperatures. In each case the

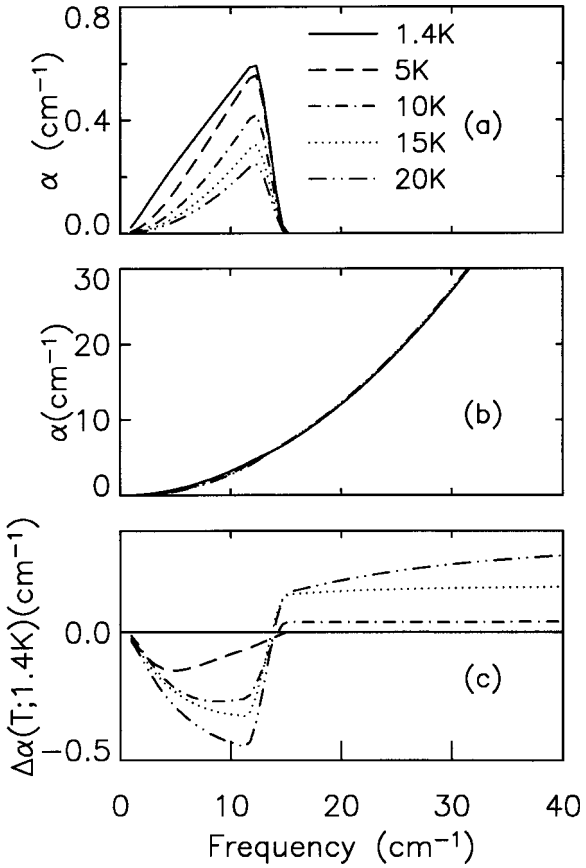

Figure 14. Theoretical predictions for a TLS model with a sharp cutoff in the TLS density of states at 13 cm^{-1}. The glass parameters are the same as those used in figure 1. (a) The absolute absorption for the resonant TLS process at 1.4, 5, 10, 15 and 20 K. (b) The total absorption including the temperature-independent absorption contribution. (c) The temperature-induced change in absorption including both resonant and relaxation terms.

nature of the temperature dependence is similar. All of our glass and mixed crystal samples (see figures 4 and 5) have a temperature-dependent absorption which decreases with increasing temperature at low frequencies, but increases at higher frequencies, with a unique frequency in the middle showing almost no temperature dependence. The results, shown in figures 5 and 6, reveal that the zero-crossing frequency is also nearly concentration independent. It appears that the temperature-dependent TLS absorption strength of all our systems scales with concentration over a significant concentration regime and that each mixed crystal system exhibits its own particular TLS frequency dependence which is largely independent of concentration.

For frequencies below 10 cm^{-1} the temperature-dependent absorption of the fluorite mixed crystal systems, $(AF_2)_{1-x}$:$(RF_3)_x$, is dominated by a distribution of the TLS. Do these TLS density of states compare to those of a glass? The last column in table 1 lists the saturated values for $n_e\mu^2$ evaluated at 6 cm^{-1}. These vary from 5×10^{-4} for the $(SrF_2)_{1-x}$:$(LaF_3)_x$ system to a maximum of 7.5×10^{-3} for the $(CaF_2)_{1-x}$:$(YF_3)_x$ system. The SLS glass has an intermediate value of 2.0×10^{-3}. In comparison, dielectric studies at 0.3 cm^{-1} obtained on a series of standard glasses produce a range for $n_e\mu^2$ from 1×10^{-3} to 4×10^{-6} [35].

(A direct comparison with these results will give slightly different values since these authors apparently did not include the local field correction in their analysis.)

The factor of 15 spread in our results for $n_e\mu^2$ will be at least partially due to a variation in the dipole moment from one fluorite mixed crystal system to the next. To make an order of magnitude estimate for the density of states of the TLS a transition dipole moment $\mu = 1D$ is assumed. This yields values of n_e varying from 5×10^{32} to 7×10^{33} erg^{-1} cm^{-3}, in good agreement with the TLS density of states for standard glasses deduced from thermal measurements, which vary from 4×10^{32} to 3×10^{33} erg^{-1} cm^{-3} [2, 5]. Incorporating our measured value for the high-frequency cutoff ranging between 10 and 20 cm^{-1} for TLS, the TLS number density is estimated to be of the order of 10^{18}–10^{19} cm^{-3}. This would imply that our strongest absorbing system, $(CaF_2)_{1-x}$:$(YF_3)_x$, has roughly one active tunnelling site for every 10^3 Y^{3+} dopant ions.

6.2. Influence of clusters on TLS

Clusters are a necessary feature of mixed crystals, but do such clusters play a special role in the far-infrared properties of TLS? Even in the earliest studies of TLS in fluorite mixed crystals it was speculated that the TLS are coupled to cluster formation [14, 15]. Recently, it has been argued by Carruzzo *et al* [36] that the formation of clusters is critical for TLS in glasses since clusters of defects lead to randomly spaced energy levels with random matrix elements connecting them [37] and at low temperatures the low-lying energy levels could act like TLS.

The fact that $G(\omega)$ saturates at the lowest dopant concentration for CaF_2 followed by SrF_2 and then BaF_2 systems could be taken as consistent with the observation that the CaF_2 host forms complex clusters at the lowest concentrations, followed by SrF_2 and then BaF_2 [31, 38, 39]. Since high-temperature thermal cycling is known to effect the formation of complex clusters in some fluorite mixed crystals [40–43] it provides another experimental parameter that can be varied. Of the six different systems studied here only $(CaF_2)_{1-x}$:$(YF_3)_x$ and $(CaF_2)_{1-x}$:$(LuF_3)_x$ showed a change in absorption as a result of heat treatment and the former was investigated in some detail [17]. For a 5 mol% Y^{3+} sample quenched from 900 °C both the far-infrared harmonic absorption and the TLS contribution were approximately a factor of two smaller than for the same sample cooled slowly from 625 °C. The fact that both the impurity-induced absorption and the TLS absorption scaled together, could simply signify that cluster formation was inducing a larger transition dipole moment for the dynamical system and that the dipole moment also made the TLS more infrared active. (Note that such impurity-induced TLS optical activity has been observed for OH-doped SiO_2 glass [35].) Hence the observed optical change does not necessarily imply that the density of the TLS has changed. For higher dopant concentrations the difference induced by the two heat treatment methods became less significant.

In another far-infrared study of a $(BaF_2)_{0.9}$:$(YF_3)_{0.1}$ sample, both the impurity-induced absorption coefficient and the TLS temperature-dependent component were found to be more than 20 times smaller than those found in $(CaF_2)_{0.9}$:$(YF_3)_{0.1}$. The fact that both components changed together could again be associated with a change in the dipole moment rather than a signature of cluster importance.

If clusters represent the sole origin of TLS behaviour then the $(BaF_2)_{1-x}$:$(LaF_3)_x$ system, which does not form clusters very readily, would be predicted to have the smallest TLS of the three hosts; but at large concentrations a larger temperature-induced change in absorption is measured for the $(BaF_2)_{1-x}$:$(LaF_3)_x$ system than for either the $(SrF_2)_{1-x}$:$(LaF_3)_x$ or $(CaF_2)_{1-x}$:$(LaF_3)_x$ systems. Similarly, the fact that other systems that form clusters do

not show any evidence for TLS [44] is also inconsistent with a direct link between cluster formation and the existence of TLS. Finally, specific cluster arrangements have been identified in the $(BaF_2)_{1-x}$:$(LaF_3)_x$ system for large x by means of neutron scattering; however, the jump frequencies are so small (<75 MHz) at elevated temperatures [45] that they cannot be important for the formation of the low-temperature far-infrared TLS. Perhaps most relevant from this far-infrared study is the fact that all the $(AF_2)_{1-x}$:$(RF_3)_x$ mixed crystal systems examined exhibit a broad distribution of TLS, with a frequency range only weakly dependent on x. This experimental fact strongly suggests that no one particular defect or cluster structure is responsible for the glass-like behaviour.

6.3. Thermal conductivity plateau in glasses

All of the low-frequency results are consistent with the low-temperature properties of the fluorite mixed crystals being classified as truly glass like. They not only indicate that these crystals have a comparable density of states of the TLS to that of a standard glass, but they also show that the density deduced from far-infrared measurements is comparable to that determined from thermal measurements obtained at an order or two orders of magnitude lower energy. So far, thermal measurements have only been able to establish the existence of TLS for temperatures below about 1 K. However, one characteristic signature at higher temperatures is a plateau in the temperature dependence of the thermal conductivity for amorphous systems. It occurs at about 12 K for silica [46]. This feature is still unexplained, although various ideas have been put forward such as fractons [47], a large interaction between TLS [37], an increase in Raleigh scattering [48, 49], or a sudden variation in the TLS density of states [50, 51].

Based on the mixed crystal TLS far-infrared data described above it would appear that the plateau may be a consequence of the resonance scattering of thermal phonons by the excited-state transitions associated with TLS. Since a black-body distribution of phonons is the source of energy transport in a thermal conductivity measurement of an insulator, the dominant scattering will occur when the peak of the phonon black-body spectrum matches the resonant frequency of the scatterer. From Wien's displacement law $\hbar\omega_m/kT \approx 3$, so that a scattering temperature of 12 K in a thermal conductivity against temperature plot corresponds roughly to a frequency of 25 cm^{-1} for the actual scattering frequency. Figure 9(b) shows that for the SLS glass the maximum for the excited-state transitions is centred at about 28 cm^{-1}. This agreement between these two frequency values suggests that resonant phonon scattering from the excited-state transitions of TLS may account naturally for the universal plateau observed in the thermal conductivity of glasses. This observation puts added restrictions on the parameters that can be used in the standard TLS tunnelling model.

6.4. Comparison to Raman measurements of TLS

The TLS spectrum of $(AF_2)_{1-x}$:$(LaF_3)_x$ where A = Ca^{2+}, Sr^{2+} or Ba^{2+} for $0 \leqslant x \leqslant 0.45$ also has been measured using Raman scattering [52], and a number of interesting properties have been found, as follows.

(a) Of the three Raman-active symmetry types present in the fluorite crystal these TLS display only A_{1g} symmetry, not E_g nor T_{2g}.
(b) In addition, there is no experimental evidence of Raman-active excited-state transitions for the TLS.
(c) The cutoff frequency of the Raman-active TLS spectrum is about the same as that observed for the far-infrared results and independent of the La^{3+} concentration.

(d) The number density of the TLS for the CaF_2 host saturates with increasing La^{3+} concentration ($\sim 5 \times 10^{18}$ cm^{-3} for CaF_2:LaF_3).

(e) The largest TLS effect is observed for the CaF_2 host and the smallest for the SrF_2 host.

(f) The low-temperature line shape of the first-order Raman-allowed T_{2g} optic mode in these mixed fluorite crystals is quite similar to those previously found for the pure systems at high temperatures [53].

(g) The largest amount of crystal disorder is observed for the La-doped CaF_2 host and the smallest for the SrF_2 host.

(h) La^{3+} is required to produce TLS since none are observed for $(A'F_2)_{1-x}$:$(AF_2)_x$ where A, $A' = Ca^{2+}$, Sr^{2+} or Ba^{2+}.

(i) The TLS number density is controlled by the law of mass action with the 'effective' temperature determined by the frozen-in lattice disorder. This leads to an absence of TLS below a certain dopant concentration.

(j) The Boson peak in Raman scattering is proportional to the impurity-induced phonon scattering while the TLS scattering is not.

When comparing the far-infrared and the Raman results it is clear from items (a), (b) and (i) that the far-infrared and Raman probe somewhat different TLS. Most intriguing is the fact that the far-infrared technique shows a TLS density of states that increases linearly with dopant concentration even at the lowest concentrations, while the Raman (and also persistent hole burning measurements [54]) show a definite absence of TLS at low, but non-zero, concentrations. A possible clue to this behaviour is that the two systems, $(CaF_2)_{1-x}$:$(LaF_3)_x$ and $(CaF_2)_{1-x}$:$(YF_3)_x$, which contain far-infrared tunnelling transitions at such low dopant concentrations also show sharp impurity-like modes and these sharp modes also exhibit the characteristic two-level temperature dependence.

The fact that the cutoff frequency is about the same for both far-infrared and Raman measurement techniques (item (c)) and that this cutoff remains unchanged, independent of La^{3+} concentration (or disorder), is a significant experimental find. A recurring theme in mixed crystal studies offered to account for a distribution of TLS is that random strains build up as the defect density increases, producing an ever widening spectrum of potential minima between which atoms can tunnel [55–57]. However, the width of such a strain-driven TLS spectrum should vary with the disorder, an effect not observed in the far-infrared data presented here nor consistent with the Raman results outlined in item (c) above. According to items (d), (e) and (i) it is only the magnitude of the TLS spectrum that depends on disorder. Item (h) is observed both in far-infrared and Raman studies, the charge mismatch brought about by doping with La^{3+} is a necessary component for the production of TLS. Substitutional lattice disorder can increase this TLS number density once the catalytic-like La^{3+} defect is present in the lattice.

7. Summary

Whereas previous workers have focused their efforts on measuring the low-frequency end of the TLS distribution, in the work reported here the high-frequency end of the TLS has been measured for different mixed fluorite crystals and for different dopants. The major findings are summarized below.

(1) All six of the fluorite mixed crystal systems of the form $(AF_2)_{1-x}$:$(RF_3)_x$ that have been examined in the far-infrared contain a broad distribution of TLS below 10–20 cm^{-1}.

(2) The effective optical density of states of TLS in the $(AF_2)_{1-x}$:$(RF_3)_x$ mixed crystals ranges from a fifth of that of a typical SLS glass for $(SrF_2)_{1-x}$:$(LaF_3)_x$ to almost five times that for $(CaF_2)_{1_x}$:$(LuF_3)_x$ and $(CaF_2)_{1-x}$:$(YF_3)_x$.
(3) The three host systems of CaF_2, SrF_2 and BaF_2 doped with LaF_3 each contain an effective density of states of the TLS which increases linearly with dopant concentration at small values and reaches saturation level at a value comparable to that of a standard glass.
(4) The fact that the width of the TLS spectrum for a given host does not change with dopant concentration argues against the hypothesis that defect strain produces an ever widening spectrum of potential minima between which atoms can tunnel.
(5) For the most strongly absorbing mixed crystal samples approximately one in every thousand dopant ions participates in (or contributes to) the TLS phenomenon.
(6) Substitutional disorder alone is not sufficient to produce TLS in the fluorite mixed crystals; a charge mismatch, or one of its consequences such as the presence of charge compensating ions or ion vacancies, is necessary.
(7) The two mixed crystals and one standard SLS glass studied at frequencies up to 40 cm^{-1} display an excited-state TLS manifold above the ground-state TLS manifold.
(8) The energy scale of these excited states provides a natural resonant phonon scattering explanation for the universal thermal conductivity plateau found in the temperature dependence of the thermal conductivity of all glasses.

Acknowledgments

We have benefited from discussions with R H Silsbee. This work is supported by NSF-DMR-9979483, NASA-MAG5-9140 and NASA-NAG8-1666.

References

[1] Zeller R C and Pohl R O 1971 *Phys. Rev.* B **4** 2029
[2] Phillips W A (ed) 1981 *Amorphous Solids* (Berlin: Springer)
[3] Hunklinger S and Raychaudhuri A K 1986 *Progress in Low Temperature Physics* ed D F Brewer (Amsterdam: North-Holland) p 265
[4] Phillips W A 1987 *Rep. Prog. Phys.* **50** 1657
[5] Berret J F and Meissner M 1988 *Z. Phys.* B **70** 65
[6] Agladze N I, Sievers A J, Jones S A, Burlitch J M and Beckwith V W 1996 *Astrophys. J.* **462** 1026
[7] Esquinazi P 1998 *Tunneling Systems in Amorphous and Crystalline Solids* (Berlin: Springer)
[8] Phillips W A 1972 *J. Low Temp. Phys.* **7** 351
[9] Anderson P W, Halperin B I and Varma C M 1972 *Phil. Mag.* **25** 1
[10] Leggett A J 1991 *Physica* B **169** 322
[11] Walker F J and Anderson A C 1984 *Phys. Rev.* B **29** 5881
[12] Sethna J P and Chow K S 1985 *Phase Transitions* **5** 317
[13] Watson S K, Cahill D G and Pohl R O 1989 *Phys. Rev.* B **40** 6381
[14] Kazanskii S K 1985 *JETP Lett.* **41** 224
[15] Cahill D G and Pohl R O 1989 *Phys. Rev.* B **39** 10 477
[16] FitzGerald S A, Campbell J A and Sievers A J 1994 *Phys. Rev. Lett.* **73** 3105
[17] FitzGerald S A, Campbell J A and Sievers A J 1996 *J. Non-Cryst. Solids* **202** 165
[18] Tu J, FitzGerald S A, Campbell J A and Sievers A J 1996 *J. Non-Cryst. Solids* **202** 153
[19] Sievers A J, Tu J J, Agladze N I, FitzGerald S A and Campbell J A 1998 *Physica* B **244** 159
[20] Topp K A, Thompson E and Pohl R O 1999 *Phys. Rev.* B **60** 898
[21] Vinogradov V S 1960 *Sov. Phys. Solid State* **2** 2338
[22] Bagdade W and Stolen R 1968 *J. Phys. Chem. Solids* **29** 2001
[23] Schlömann E 1964 *Phys. Rev.* **135** A413
[24] Bösch M A 1978 *Phys. Rev. Lett.* **40** 879
[25] Strom U, Hendrickson J R, Wagner R J and Taylor P C 1974 *Solid State Commun.* **15** 1871

[26] Hunklinger S and von Schickfus M 1981 *Amorphous Solids: Low-Temperature Properties* ed W A Phillips (Berlin: Springer) p 83
[27] Hayes W and Stoneham A M 1974 *Crystals with the Fluorite Structure* ed W Hayes (Oxford: Clarendon)
[28] Roth R S, Negas T and Cook L P 1981 *Am. Ceram. Soc. Bull.* **60** 376
[29] Love S P, Ambrose W P and Sievers A J 1989 *Phys. Rev.* B **39** 10 352
[30] FitzGerald S A, Campbell J A and Sievers A J 2001 *J. Phys.: Condens. Matter* **13**
[31] den Hartog H W 1994 *Defects and Disorder in Crystalline and Amorphous Solids* ed C R A Catlow (London: The Royal Institute of Great Britain) p 435
[32] Mon K K, Chabal Y C and Sievers A J 1975 *Phys. Rev. Lett.* **35** 1352
[33] See appendix A in Alexander R W, Hughes A E and Sievers A J 1970 *Phys. Rev.* B **1** 1563
[34] Kirby R D, Hughes A E and Sievers A J 1970 *Phys. Rev.* B **2** 481
[35] von Schickfus M and Hunklinger S 1976 *J. Phys. C: Solid State Phys.* **9** L439
[36] Carruzzo H M, Grannan E R and Yu C C 1994 *Phys. Rev.* B **50** 6685
[37] Yu C and Legget A J 1988 *Comments Cond. Matter Phys.* **14** 231
[38] Andeen C G, Fontanella J J, Wintersgill M C, Welcher P J, Kimble R J and Mathews G E 1981 *J. Phys. C: Solid State Phys.* **14** 3557
[39] Bendall P J, Catlow C R A, Corish J and Jacobs P W M 1984 *J. Solid State Chem.* **51** 159
[40] Tallant D R, Moore D S and Wright J C 1977 *J. Chem. Phys.* **67** 2897
[41] Moore D S and Wright J C 1981 *J. Chem. Phys.* **74** 1626
[42] Jacobs P W M and Ong S H 1979 *J. Phys. Chem. Solids* **41** 431
[43] Ong S H and Jacobs P M 1980 *J. Solid State Chem.* **32** 193
[44] Nair I R and Walker C T 1972 *Phys. Rev.* B **5** 4101
[45] Andersen N H, Clausen K N, Kjems J K and Schoonman J 1986 *J. Phys. C: Solid State Phys.* **19** 2377
[46] Elliott S R 1990 *Physics of Amorphous Materials* (New York: Wiley)
[47] Orbach R 1986 *Science* **231** 814
[48] Graebner J E, Golding B and Allen L C 1986 *Phys. Rev.* B **34** 5696
[49] Freeman J J and Anderson A C 1986 *Phonon Scattering in Condensed Matter* vol V, ed A C Anderson and J P Wolfe (Berlin: Springer) p 32
[50] Yu C C and Freeman J J 1987 *Phys. Rev.* B **36** 7620
[51] Grannen E R, Randeria M and Sethna J P 1988 *Phys. Rev. Lett.* **60** 1402
[52] Tu J J and Sievers A J 1999 *Phys. Rev. Lett.* **83** 4077
[53] Elliott R J, Hayes W, Kleppmann W G, Rushworth A J and Ryan J F 1978 *Proc. R. Soc.* A **360** 317
[54] Love S P, Mungan C E, Sievers A J and Campbell J 1992 *J. Opt. Soc. Am.* B **9** 794
[55] Watson S K 1995 *Phys. Rev. Lett.* **75** 1965
[56] Liu X, Vu P D, Pohl R O, Schiettekatte F and Rooda S 1998 *Phys. Rev. Lett.* **81** 3171
[57] Pohl R O, Liu X and Crandall R S 1999 *Solid State Mater. Sci.* **4** 281